Deposition of vanadium oxide films by direct-current magnetron reactive sputtering

E. Kusano,[a] J. A. Theil, and John A. Thornton
Department of Materials Science and Coordinated Science Laboratory, University of Illinois, Urbana, Illinois 61801

(Received 28 September 1987; accepted 9 November 1987)

Vanadium dioxide is well known for the semiconductor–metal phase transition at 67 °C which has yielded resistivity changes as high as 10^5 in single crystals. Our objective is to demonstrate that thin films with high transition resistivity ratios can be deposited at modest substrate temperatures by dc reative sputtering from a vanadium target in an O_2–Ar working gas using a planar magnetron source, because of the capabilities of this method for depositing large-area thermal control surfaces. We have obtained resistivity ratios of $\sim 5 \times 10^3$, between a semiconductor phase with a resistivity of $\sim 5\ \Omega$ cm, and a metallic phase with a resistivity of $\sim 10^{-3}\ \Omega$ cm for films deposited onto borosilicate glass substrates at ~400 °C. X-ray diffraction showed the films to be single-phase VO_2 with a monoclinic structure. The VO_2 films are obtained for a narrow range of O_2 injection rates which correspond to conditions where cathode poisoning is just starting to occur, i.e., where the sputtered flux of vanadium, as measured by *in situ* optical emission spectroscopy, is decreasing and the oxygen partial pressure is increasing. Higher or lower injection rates, for a given discharge current, give films with unfavorable stoichiometry and/or structure and lower resistivity ratios during the transition.

I. INTRODUCTION

Vanadium dioxide is well known for its semiconductor-to-metal transition at 67 °C which has yielded resistivity changes as large as 10^5 in single crystals.[1] This transition is a result of a structural change from a monoclinic to a tetragonal rutile lattice. The electronic transition involves the vanadium *d*-shell electrons. The generally accepted model was proposed by Goodenough.[2] The oxygen $2s2p_\sigma^2$ orbitals and the vanadium $3d_\sigma^2 4s4p_\sigma^3$ orbitals combined to form cation–anion bonding and antibonding orbitals. The crystalline field completely removes the *d*-state degeneracy. Thus the two e_g orbitals are split into two d_σ orbitals, that participate in the bonding as noted above. The three t_{2g} orbitals split into d_π orbitals, which mix with the anion p_π orbitals and a $d_\parallel$ orbital to form a set of levels separated by ~2 eV from the valence band. In the high-temperature metal phase these levels (the $d_\pi - p_\pi$ and $d_\parallel$ states) overlap to form a band within which the Fermi level is located. In the structure change associated with the formation of the low-temperature monoclinic semiconducting phase, the slight shift in vanadium atom nearest-neighbor distances splits this band into the subbands, one containing the $d_\pi - p_\pi$ states, and one containing the $d_\parallel$ states, thereby creating a band gap of ~0.7 eV within which the Fermi level is located. The low-temperature semiconducting phase in single crystals exhibits *n*-type conductivity with a resistivity ρ_s of $\sim 10\ \Omega$ cm, Hall mobility of ~0.5 $cm^2/V\,s$ and activation energy for conduction of ~0.5 eV. The *d*-shell charge carriers are believed to be heavy polarons.[3] The high-temperature metallic phase in the best single crystals exhibits a resistivity ρ_m of $\sim 10^{-4}\ \Omega$ cm, a positive temperature coefficient of resistance (TCR), and a comparable mobility—i.e., the primary effect of the transition is to increase the number of charge carriers.[4,5]

The deposition of thin films of VO_2 with high transition resistivity ratios (ρ_s/ρ_m) requires deposition procedures that yield films with a minimum density of band-gap states in the semiconductor phase and a low resistivity in the metallic phase. The deposition problem is exacerbated by the fact that the desired VO_2 phase is surrounded by nine other phases, i.e., V_2O_3, V_3O_5, V_4O_7, V_5O_9, V_6O_{11}, V_7O_{13}, V_3O_7, and V_2O_5.[6] Resistivity ratios between 10^3 and 10^4 have been obtained for VO_2 films deposited onto sapphire substrates by dc planar diode reactive sputtering,[7,8] rf planar diode reactive sputtering,[9] reactive ion beam sputtering,[10] ion-assisted reactive evaporation and annealing,[11] and reactive evaporation.[12]

We have been investigating VO_2 deposition by dc planar magnetron reactive sputtering because the large-area capabilities of this method suggest that it might be suitable for depositing thermal control coatings[13] and because the complexity of V–O phase diagram provides an excellent vehicle for investigating the reactive sputtering process. This paper reports the influence of deposition conditions on the structure and properties of VO_x coatings deposited at moderate temperatures ($\leqslant$500 °C) onto glass substrates. The effects of annealing are also discussed.

II. FILM DEPOSITION

Figure 1 shows a schematic drawing of the experimental apparatus. The sputtering source is a circular planar magnetron configured for mounting 12.7-cm-diam targets. The target was a 99.997% pure vanadium plate (Teledyne Wah Chang, Albany, OR) solder bonded to a water-cooled Cu backing plate. The substrates were $25 \times 25 \times 1.6$ mm borosilicate glass plates (Corning type 7059), which were introduced through a load lock and inserted into a substrate holder containing two tungsten/quartz infrared (IR) heating lamps. Substrate temperatures were estimated using a dummy glass substrate with an embedded Chromel–Alumel

 0734-2101/88/031663-05$01.00

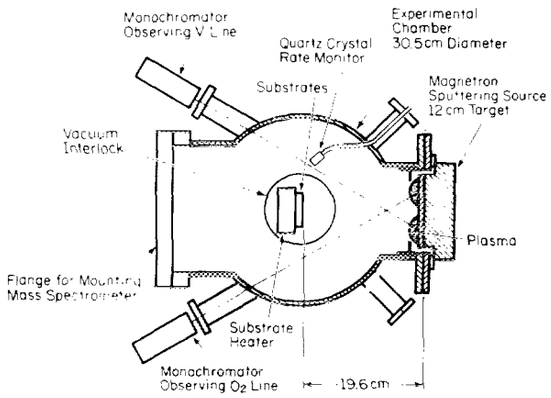

FIG. 1. Schematic illustration of deposition apparatus.

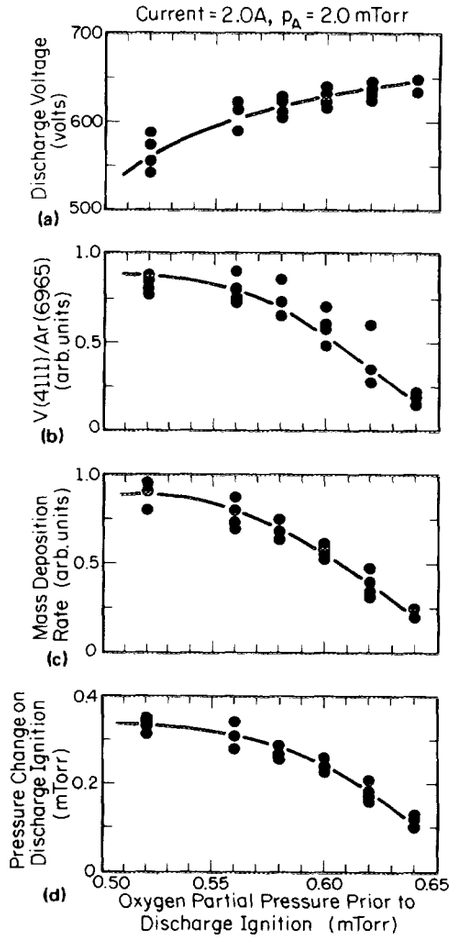

FIG. 2. Variation of (a) discharge voltage, (b) atomic line emission from sputtered vanadium atoms relative to line emission from argon plasma, (c) mass deposition rate, and (d) pressure change during discharge ignition (oxygen consumption), with oxygen partial pressure prior to discharge ignition (oxygen injection rate) for the reactive sputtering conditions used in this paper.

thermocouple, which was calibrated by placing substrates with embedded thermocouples in the deposition positions and coating them with VO_2 to account for emissivity effects. The working gases were Ar (99.999%) and O_2 (99.998%), which were injected separately through Tylan type FC 260 electronic mass flow controllers. The total pressure was measured with an MKS type 310BHS capacitive manometer. Pumping was provided by a throttled Freon-trapped oil diffusion pump. The pumping speed S for O_2 at the deposition conditions was about 230 l/s. Predeposition vacuums were in the 10^{-6} Torr (10^{-4} Pa) range. Deposition rates were monitored with an Inficon quartz-crystal rate detector. The sputtered vanadium flux was monitored by measuring the emission from the V I-4111 Å line in the plasma region over the sputtering target. Variations in the excitation function were largely accounted for by using a second monochromator to simultaneously measure the emission from the Ar I-6965 Å line.

This paper reports film properties as a function of the O_2 injection rate, for substrate temperatures in the 300–500 °C range, while using a constant Ar pressure of 2.0 mTorr and discharge current of 2.0 A. Presputtering was done for ~10 min at each deposition condition with the substrates shielded. Coating thicknesses were between 400 and 700 nm. Figure 2 shows the variation in the discharge voltage, normalized V line emission, mass deposition rate, and pressure change Δp on discharge ignition, as a function of the oxygen partial pressure p_{O_2} prior to discharge ignition over the experimental range covered in this paper. (Note that $p_{O_2}S$ is the oxygen injection rate and ΔpS is the total oxygen consumption in the deposition reaction.) Since the discharge voltage increased with p_{O_2}, a constant current dc power supply was used to provide stable operation in the region of target oxidization.

The variation of discharge operating conditions with oxygen injection rate was typical of that for a system undergoing target poisoning.[14] Thus at a given discharge current and Ar pressure four operating regions could be identified with respect to variations in the oxygen injection rate.[15] At modest oxygen injection rates, $p_{O_2} < \sim 0.3$ mTorr for the conditions of the experiments reported here ($p_{Ar} = 2.0$ mTorr, current = 2.0 A), the oxygen consumption was complete within a geometric factor relating to the physical and getter pumping speeds. In this region the target surface and the vanadium sputtering are not significantly affected by the oxygen injection. At higher p_{O_2} ~0.3–0.5 mTorr for the conditions of our experiments) we observed the onset of target surface reactions, with an associated increase in discharge voltage, and decrease in the sputtered V flux (normalized V line emission), mass deposition rate, and oxygen consumption. For p_{O_2} between ~0.5 and 0.7 mTorr, evidence of significant target surface reactions (poisoning) is seen, with more dramatic increases in discharge voltage and decreases in the vanadium sputtering rate, mass deposition rate, and oxygen consumption. It is this region, where the system is in a delicate state of balance between wall and target surface reactions, that is shown in Fig. 2 with a rather expanded p_{O_2} scale. The oxide phases detected by x-ray diffraction in this region are summarized in Fig. 3. They vary from V_2O_3 to V_2O_5. Thickness deposition rates varied from ~30 to ~10 nm/min. At higher O_2 injection rates ($p_{O_2} > 0.7$ mTorr for

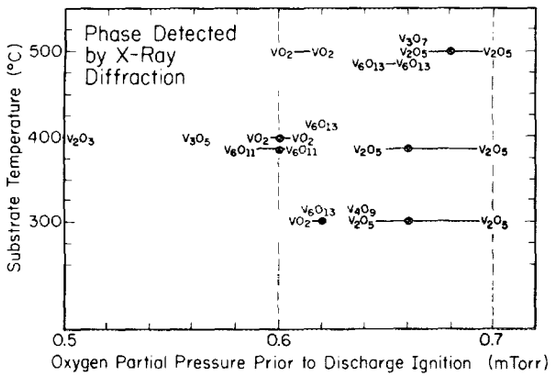

FIG. 3. Major phases identified by x-ray diffraction in reactive sputtered vanadium oxide coatings as a function of the deposition conditions. The black data points identify additional conditions under which the phase indicated was identified.

our conditions) the target poisoning was apparently complete and the deposition conditions were relatively constant.

III. FILM PROPERTIES

It was possible to deposit single-phase VO_2 films (within the limits of x-ray diffraction) at elevated substrate temperatures (400–500 °C) over a limited range of O_2 injection rates, as summarized in Fig. 3. We cannot exclude the presence of minority phases in small amounts because of the preferred orientation that was found in the films. The films deposited at 300 °C were not single phase and yielded low resistivity ratios ($< 10^2$) at all oxygen partial pressures. However, at 400 °C we obtained single-phase $<011>$ oriented VO_2 films with resistivity ratios in the 10^3–6×10^3 range. The sensitivity to oxygen injection rate is shown by the resistivity data given in Fig. 4. Films deposited at 500 °C in 0.60–0.62 mTorr partial pressure range appeared to be single-phase VO_2 but yielded lower resistivity ratios ($< 10^3$).

A typical resistivity hysteresis curve is shown in Fig. 5. The sample was deposited at 400 °C using an optimized O_2 injection rate (p_{O_2} slightly higher than 0.60 mTorr). The conductivity in the semiconductor phase exhibits an activation energy of ~0.2 eV. The metal phase resistivity appears to be constant, but may involve a slightly negative temperature coefficient of resistance. The transition width is ~10 °C. The hysteresis widths (defined at the midpoint of the transition) were typically 2–3 °C in our samples.

It has long been recognized that grain structure, as well as stoichiometry and crystallographic phase, contribute to the resistivity ratio in VO_2 thin films.[8,10,16] Figure 6 shows scanning electron microscope (SEM) micrographs of the surface topography for films deposited under various conditions. Fracture cross sections confirmed that the films which yielded the highest resistivity ratios [$p_{O_2} \approx 0.60$ mTorr, $T_s = 400$ °C, Fig. 6(c)] possessed a columnar structure defined by voided boundaries having feature sizes of 100 nm or less. Lower temperatures [Fig. 6(f)] yielded films with smooth surfaces and featureless fracture cross sections. Higher temperatures [Fig. 6(a)] yielded larger, highly faceted grains (typically 250 nm in size) which were poorly

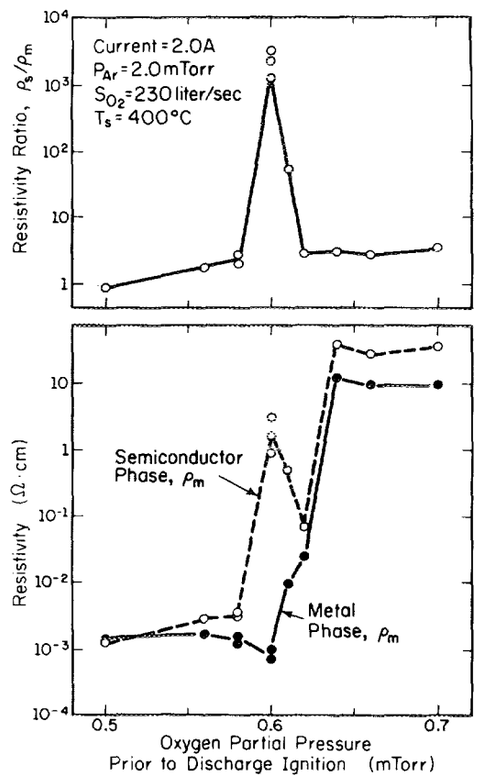

FIG. 4. Coating resistivity variation vs oxygen injection rate for measurements made below the transition temperature (semiconductor phase) and above the transition temperature (metal phase). Coatings were deposited onto glass substrates at the substrate temperature (400 °C) that yielded the highest resistivity ratios.

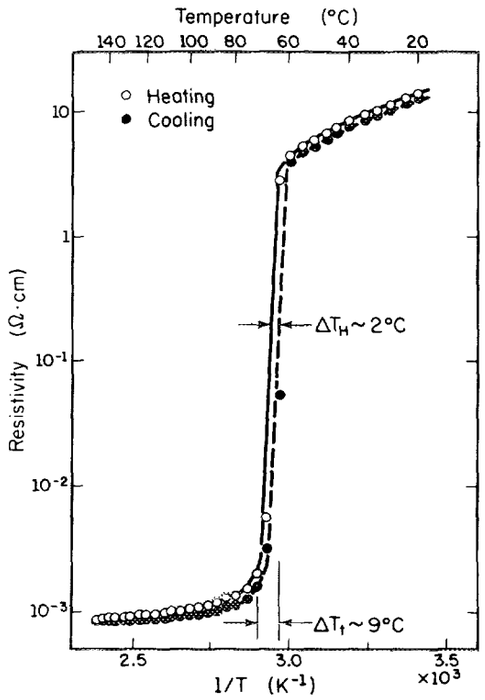

FIG. 5. Resistivity variation that was measured as one of the coatings with a high as-deposited resistivity ratio was passed through the structure transition.

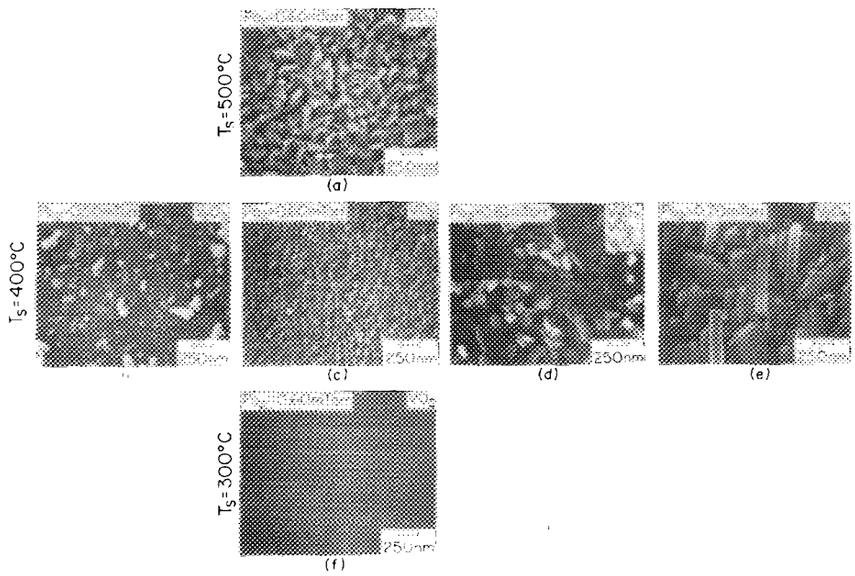

FIG. 6. Scanning electron micrographs showing the variations in surface topography that were found for coatings deposited onto glass substrates at the conditions indicated. The coatings were nominally 500 nm thick. The highest as-deposited resistivity ratios were found for coatings deposited under the conditions listed for (c).

connected. Slight increases in oxygen partial pressure at 400 °C yielded an abrupt change in the surface roughness [Fig. 6(d)], and at higher partial pressures [Fig. 6(e)], V_2O_5 films with a high degree of preferred orientation and relatively large anisotropic grains. The voided boundaries seen in Fig. 6(c) are typical of those found when atomic shadowing plays a role in the development of the microstructure.[17] The degree of crystallization and the particular phases present within the films can be expected to influence the surface morphology and the development of shadow induced voided boundaries. This may explain the differences between Figs. 6(f) and 6(c).

IV. DISCUSSION

The thin-film structure appears to have only a second-order influence on the occurrence of a transition in the atomic bonding orbitals. Thus a broad temperature-induced transition ($\Delta T \sim 50$ °C) in the optical properties of amorphous samples which is typical of the phase transition in VO_2, has been reported.[16] This is perhaps to be expected because of the localized nature of the participating *d*-shell orbitals. However, the manifestation of such a transition in terms of a large resistivity ratio requires structure perfection, i.e., the highest possible semiconductor resistivity ρ_s and the lowest possible metal phase resistivity ρ_m. Our best films have yielded ρ_s in the 1–3 Ω cm range, i.e., a factor of 3 to 10 below that of the best single-crystal data, and ρ_m in the 5×10^{-4}–10^{-3} Ω cm range, which is 5 to 10 times larger than one finds in the best single crystals.[1] Preliminary transmission/reflectance and photothermal deflection measurements suggest that the defect states in the band gap are the source of the reduced ρ_s. The voided columnar boundaries are believed to be the origin of the increased ρ_m. The rounding at the high-temperature end of the transition (Fig. 5), and the hint of a negative TCR, may signal an intergrain phase which forces current flow to be by tunneling.

Case has reported obtaining ρ_s values in the single-crystal range ($\sim$10 Ω cm) by postdeposition annealing polycrystalline films on sapphire substrates at 520 °C in 1.5–3.5 mTorr of oxygen for 1.5 h.[11] The data in Fig. 6 suggest that the structural transition with increasing O_2 partial pressure may have precluded the deposition of coatings with reduced oxygen vacancy levels and high ρ_s. Terukov *et al.* have reported evidence that a deficiency of oxygen raises the carrier density in the semiconductor phase and reduces the resistivity ratio.[18] Accordingly experiments were conducted in which coatings were deposited at $p_{O_2} = 0.60$ mTorr and various substrate temperatures, and then annealed *in situ* at 400 °C in 2 mTorr of oxygen for various periods up to 45 min prior to their removal from the chamber. The data in Fig. 7 show that ρ_s equal to the single-crystal values of 10 Ω cm were indeed achieved by this method along with resistivity ratio increases by a factor of 3 to 5.

Nyberg and Buhrman have investigated the optical properties of films deposited at various substrate temperatures and oxygen partial pressures onto sapphire substrates by electron beam reactive evaporation.[12] At typical deposition rates (3 nm/min), coatings deposited at 500 °C and 1 mTorr of O_2 yielded optical and electrical properties typical of those commonly reported in previous thin-film work. In the semiconducting phase the optical absorption increased gradually near 0.5 eV, suggesting sub-band-gap absorption, and exhibited a pronounced shoulder at $\sim$2 eV which may be due to the valence band to *d*-shell transition discussed in the introduction. Optical absorption measurements examining the semiconductor phase of our best films exhibit a virtually identical behavior. It is interesting to note that at a higher substrate temperature (590 °C) and oxygen partial pressure (12 mTorr) (i.e., conditions that would be expected to yield a higher oxygen-to-vanadium flux ratio and a reduced oxygen vacancy level) Nyberg and Buhrman obtained films with high resistivity ratios ($\sim10^4$). The semiconductor

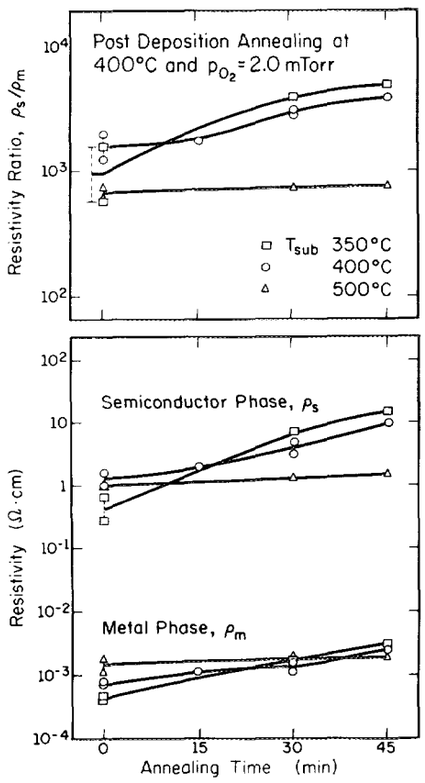

FIG. 7. Coating resistivity as a function of annealing time for measurements made below the transition temperature (semiconductor phase) and above the transition temperature (metal phase). The coatings were deposited and then annealed, for the times indicated, without breaking vacuum.

phase of these films exhibited a sharp absorption edge at ~0.5 eV suggesting reduced sub-band-gap absorption and no shoulder near 1.5 eV.

V. CONCLUSION

At the modest substrate temperature (< 500 °C) that must be used for VO_2 deposition onto glass substrates or in multilayer structures, microstructure variations along with the nonlinearities of the reactive sputtering process limit the range of oxygen partial pressures that can be used. Consequently the resistivity ratios that can be achieved in the as-deposited state are limited by electrically active defects (possibly oxygen vacancies) which restrict the resistivity of the semiconductor phase, and crystal boundaries which restrict the conductivity of the metal phase. Nevertheless as-deposited resistivity ratios in the 3×10^3 range have been achieved on glass substrates. Furthermore, postdeposition annealing can reduce the electrically active defects that influence the semiconducting phase. Therefore, there is evidence that an optimum combination of deposition and annealing conditions could yield even higher resistivity ratios at substrate temperatures not exceeding 400 °C.

ACKNOWLEDGMENTS

This work was supported by the NASA Lewis Research Center under Grant No. NAG-3-591 and by a grant from the Nippon Sheet Glass Co., Ltd.

[a] On leave from Nippon Sheet Glass Co., Ltd., Toyosato, Ibaraki, 300-26, Japan.

[1] L. A. Ladd and W. Paul, Solid State Commun. **7**, 425 (1969).
[2] J. B. Goodenough, J. Solid State Chem. **3**, 490 (1971).
[3] N. F. Mott, *Metal–Insulator Transitions* (Barnes & Noble, New York, 1974), p. 189.
[4] D. H. Hensler, J. Appl. Phys. **39**, 2354 (1968).
[5] C. C. Y. Kwan, C. H. Griffiths, and H. K. Eastwood, Appl. Phys. Lett. **20**, 93 (1972).
[6] K. Kosuge, J. Phys. Chem. Solids **28**, 1613 (1967).
[7] E. N. Fuls, D. H. Hensler, and A. R. Ross, Appl. Phys. Lett. **10**, 199 (1967).
[8] G. A. Rozgonyi and D. H. Hensler, J. Vac. Sci. Technol. **5**, 194 (1968).
[9] C. H. Griffiths and H. K. Eastwood, J. Appl. Phys. **45**, 2201 (1974).
[10] E. E. Chain, J. Vac. Sci. Technol. A **4**, 432 (1986).
[11] F. C. Case, J. Vac. Sci. Technol. A **5**, 1762 (1984).
[12] G. A. Nyberg and R. A. Buhrman, Thin Solid Films **147**, 111 (1987).
[13] W. S. Boyle and H. W. Verleuv, Appl. Phys. Lett. **12**, 28 (1968).
[14] J. A. Thornton, in *Deposition Technology (Films and Coatings for Technology)*, edited by R. F. Bunshah (Noyes, Park Ridge, NJ, 1982), pp. 170–243.
[15] J. A. Theil, E. Kusano, and J. A. Thornton (to be published).
[16] A. R. Begishev, G. B. Galiev, A. S. Ignat'ev, V. G. Mokerov, and V. G. Poshin, Sov. Phys. Solid State **20**, 951 (1978).
[17] J. A. Thornton, Annu. Rev. Mater. Sci. **7**, 239 (1977).
[18] E. I. Terukov, K.-D. Ufert, and F. A. Chudnovskii, Sov. Phys. Solid State **18**, 1450 (1976).